The (Tetraazaannulene)copper-Catalyzed Reduction of Sulfur(IV) Species. A Pulse-Radiolysis and Theoretical Study of the Associated Reaction Mechanism

by **Guillermo Ferraudi***[a])[b]), **Guillermina Estiu**[a])[c]), **A. Graham Lappin**[a]), **Manuel Villagran**[d]), **Juan P. Muena**[d]), **Juan Costamagna**[d]), and **Jose Zagal**[d])

[a]) Department of Chemistry, University of Notre Dame, Notre Dame, IN 46556, USA
[b]) Radiation Research Building, Department of Chemistry, University of Notre Dame, Notre Dame, IN 46556, USA
[c]) Walther Cancer Research Center and Department of Chemistry and Biochemistry, University of Notre Dame, Notre Dame, IN 46556-5670, USA
[d]) Facultad de Quimica y Biologia, Universidad de Santiago de Chile, Santiago-33, Chile

The monomeric species, $[Cu^{II}\{H_x(tmdnTAA)\}]^{x+}$ ($x = 0$, 1, and 2, and $(tmdnTAA)^{2-}$ = [5,7,12,14]-tetramethyldinaphtho[*b*,*i*][1,4,8,11]tetraaza[14]annulenato(2 –) = 7,9,18,20-tetramethyldinaphtho[2,3-*b*:2′,3′-*i*][1,4,8,11]tetraazacyclotetradecinato(2 –)) catalyze the electrochemical reduction of SO_2(aq) in homogeneous solution. A pulse-radiolytic study of the reaction of the $[Cu^{I}$(tetraazaannulene)] complexes with S^{IV} species revealed the formation of $Cu^{I}-SO_2$ adducts. The formation of $Cu^{I}-SO_2$ adducts prevents the disproportionation of the Cu^{I} complexes and precedes the reduction of the S^{IV} species to $S_2O_4^{2-}$. DFT Calculations were carried out to establish the structure and stability of the $Cu^{I}-SO_2$ adducts. A good agreement between the calculated and recorded electronic spectrum of the $Cu^{I}-SO_2$ adducts corroborated the formation of species with SO_2 coordinated to Cu^{I} through the O-atom.

Introduction. – In recent years, there have been an increasing interest in the design, synthesis, and use of diverse macrocyclic receptors capable of selective recognition of metal ions, anions, and neutral molecules [1 – 14], since their cavity sizes, shapes, and components can be readily modified. Among them, polyazamacrocycles have extensively been studied [2 – 7]. These compounds are able to coordinate divalent metal cations, such as Ni^{2+} or Cu^{2+}, by displacing protons of the macrocycle. The resulting complexes have many applications in catalysis [4], molecular machines, oxygen uptake [8][9][15], and medicine [8], and as antiviral agents [16 – 18], and can be even studied as biological models for metalloproteins [19]. Moreover, the structural features of the macrocycles and the unique radiophysical properties of copper radioisotopes led to their potential usefulness in diagnostic and/or therapeutic applications [20].

Copper ions in different oxidation states are present in a diverse group of metalloenzymes, in which the metal is coordinated to N-, O-, and S-atoms. In type-I Cu-centers (*e.g.*, in amicyanin, plastocyanin, and pseudoazurin), the Cu^{II} ion is coordinated in a trigonal-planar fashion by 2 histidine and 1 cysteine ligand (N_2S coordination) with one or two weakly interacting axial ligands (S or O), whereas type-II Cu-centers (*e.g.*, in dioxygenase, monooxygenases, nitrite reductase) exhibit a square-planar coordina-

tion by N or N/O ligands. S-Ligands were only detected in the diethyl dithiocarbamate inhibited form of the enzyme quercetin 2,3-monooxygenase [8][10][19][21]. S-Ligation to the metal center(s) confers specific properties to copper enzymes, and has regained importance since the discovery of the novel HisCuS(Met) center in the active site of nitrous oxide reductases [22–25]. In the presence of reactive O-species, Met can be oxidized to the corresponding sulfoxide, producing a coordination sphere that has not yet been unambiguously determined, mainly due to the ambidentate nature of sulfoxide ligands [26].

A more detailed understanding of the interaction of S^{IV} species (hydrated sulfur dioxide, hydrogen sulfite, and sulfite) with transition-metal atoms would also help to improve the efficiency of metal-catalyzed reactions, of outmost interest for their industrial and environmental applications. The use of S^{IV} in food preservation and its toxic and adverse genetic effects after exposure can be mentioned [27]. As a consequence, much of the research attention has focused on both the catalyzed autooxidation of S^{IV} to sulfate and the reduction of SO_2(aq) to $S_2O_4^{2-}$ [27–30]. The latter is catalyzed by tetraazaannulene complexes electropolymerized on a glassy carbon electrode (SO_2(aq) in a 50% (*v*/*v*) DMF/H_2O solvent) [31], and the formation of unstable complexes between the catalyst and SO_2 has been proposed for it. Nevertheless, the sparse knowledge of the kinetics and mechanism of these processes has become the limiting factor in the design of new catalysts. On the other hand, nothing is known of the catalysts of the SO_2(aq) reduction by [Cu(tetraazaannulene)] complexes in homogeneous solution, which is the target of the present research.

A previous study of the thermal and photophysical properties of the Ni^{II} and Cu^{II} complexes of [1,8]dihydro[5,7,12,14]tetramethyldinaphtho[*b*,*i*][1,4,8,11]tetraaza[14]-annulene, H_2(tmdnTAA)) and of H_x(tmdnTAA)$^{(x-2)}$ ($x = 0$ and 1) [30–32], showed that excited states localized in the naphthol moieties of the macrocycle are formed when they are irradiated at wavelengths of the near-UV bands. The complexes display acid–base equilibria (*Scheme 1*) in the ground and excited states, whose displacement causes their luminescence to be medium-dependent and accounts for transient changes in the absorption spectrum of the complexes. The chemical characteristics of the complexes make them particularly suitable to be studied by pulse-radiolysis methods. They were used in this research, together with electrochemical and computational techniques.

Experimental. – *Materials.* The *x*hydro[5,7,12,14]tetramethyldinaphtho[*b*,*i*][1,4,8,11]tetraaza[14]annulene (H_x(tmdnTAA)$^{(x-2)}$) complexes of Cu^{II} and Ni^{II} were available from previous works [31–33]. Other materials were of reagent grade and used without further purification.

Pulse-Radiolytic Procedures. The pulse-radiolysis method successfully used in a study of the mechanism of a porphyrin-complex oligomerization was used in this work [34]. Pulse-radiolysis experiments were carried out with a *TB-8/16-1S* electron linear accelerator. The instrument and computerized data collection for time-resolved UV/VIS spectroscopy and reaction kinetics have already been discussed elsewhere [35–39]. Thiocyanate dosimetry was carried out at the beginning of each experimental session. The details of the dosimetry have been reported elsewhere [35][39]. The procedure is based on the concentration of $(SCN)_2^-$ radicals generated by the electron pulse in an N_2O-sat. 10^{-2} M SCN^- soln. Doses that, in N_2-sat. aq. solns., resulted in $(2.0 \pm 0.1) \cdot 10^{-6}$ M to $(6.0 \pm 0.3) \cdot 10^{-6}$ M concentrations of e_{sol}^- were used. The solns. were deaerated with streams of the O_2-free gas, N_2 or N_2O, that was required for the generation of a given radical species. An appropriate flow of the soln. through the reaction cell was maintained during the experiment.

Scheme 1. *Ground-State Acid–base Equilibria between Complexes of* $H_x(tmdnTAA)^{(x-2)}$ (H_x(tmdnTAA)$^{(x-2)}$ = *x*hydro[5,7,12,14]tetramethyldinaphtho[*b*,*i*][1,4,8,11]tetraaza[14]annulene where *x* is the number of acidic protons). The equilibrium constants are: $K_1 = 4.5 \cdot 10^{-6}$ and $K_2 = 8.3 \cdot 10^{-9}$ for Ni^{II}, and $K_1 = 4.0 \cdot 10^{-6}$ and $K_2 = 3.9 \cdot 10^{-8}$ for $M = Cu^{II}$ [32].

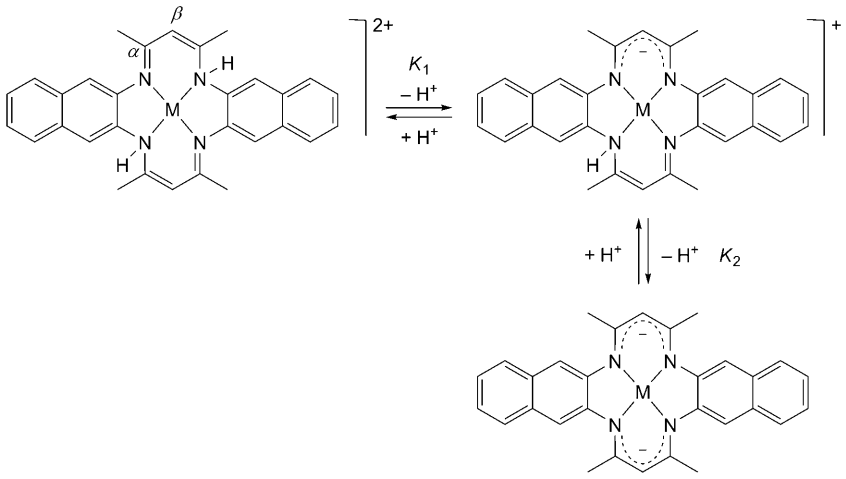

In N_2O-sat. solns. containing 0.1M MeOH or i-PrOH, the respective reactions of the radiolytically generated $OH^{\bullet}$ and $H^{\bullet}$ radicals with these alcohols produced the $C^{\bullet}H_2OH$ or $Me_2C^{\bullet}OH$ radicals [34–36]. Concentrations of the tetraazaannulene complexes (see *Results and Discussion*) were kept sufficiently low, in the order of 10^{-4} M, to prevent them from reacting with the complexes. The pH of the solns. used for pulse radiolysis was adjusted with millimolar concentrations of the acetic acid/acetate buffer (pH 5.2), and the $H_2PO_4^-/HPO_4^{2-}$ buffer (pH = 6 and 7).

The time-resolved optical changes caused by the reactions were modeled with a commercial package, Mathcad 2001i and VisSim V5. A series solution of the rate equations for the reactions described in the text were used in the calculations [34–36].

Electrochemical Experiments. The electrochemical apparatus and methods have been described in [40]. The cyclic voltammetry experiments were carried out with a *VoltaLab-PGZ-100* potentioscan along with a Voltamaster 4 software. All the voltammetric measurements were performed in a conventional three-compartments *Pyrex* cell by procedures described elsewhere [40][41a,b]. The working electrode was a glassy carbon (GCE) disk of 0.07 cm^2 exposing area. The counter electrode was a Pt coil of high area, and a Ag/AgCl electrode was used as a reference electrode. To avoid contamination of the reference electrode with S^{IV} soln., it was maintained in a hermetic tube containing KCl soln., and the *Luggin* capillary was a Pt wire.

Analytical Procedures. To detect $S_2O_4^{2-}$ in the electrolyzed solns., an anal. test was developed on the basis of the reduction of methylviologen (MV^{2+}) by $S_2O_4^{2-}$ and/or by its dissociation product $SO_2^{\bullet-}$ [42]. A 2-ml volume of the tested soln. was mixed with an equal volume of a soln. containing $2 \cdot 10^{-2}$ M MV^{2+} in a gastight spectrophotometer cell. The formation of the $MV^{\bullet+}$ radical occurring when $S_2O_4^{2-}$ is present in the soln. was investigated at 600 nm. A blank made from the nonelectrolyzed soln. was used as a reference. Insofar as O_2 promptly oxidizes $MV^{\bullet+}$, it was removed from both solns. before mixing, and they were mixed under anaerobic conditions. No other species present in the tested solns., *i.e.*, SO_3^{2-} or the tetraazaannulene complexes, interferes with the determination of $S_2O_4^{2-}$.

Computational Methods. The computational study of the Cu transition-metal complexes was carried out by the density-functional-theory (DFT) methods implemented in Gaussian 03 [43]. DFT Methods have been shown to reproduce the structural properties of several biologically interesting transition-metal centers, and their validity to model ground-state properties is widely accepted [44–48]. On this

basis, they have been used to better assess the structural characteristics of the reaction intermediates, helping in this way to discern among possible reaction mechanisms [43]. The systems studied herein were subjected to unrestrained energy minimizations by means of the B3LYP functional [44][49] with the 6-31 + G* basis set [47][50] for nonmetal atoms and the *Los Alamos* effective core potentials (LANL2DZ) [51–53] for the metal. The basis set was chosen following a recently published study of the performance of different DFT methods/basis sets for the calculation of heats of formation of different systems containing third-row transition metals [54]. To correct for the basis-set-superposition error (BSSE), the counterpoise method of *Boys* and *Bernardi* [55] was used throughout the optimization. To account for solvation entropic effects in the aq. environment, the free energies were evaluated by the calculation of the second derivatives and corrected for solvation, for the geometries previously optimized *in vacuo*. The solvent (H_2O) was modeled within a continuous approach (polarizable continuous model, PCM) [56]. Charge-transfer effects were evaluated by the calculation of the distribution of the local charges on the atoms and from the assignment of the orbitals involved in electronic transitions. Charges from electrostatic potentials (CHelpG, G03) [57] and time-dependent DFT models were used, resp.

Results and Discussion. – To determine the catalytic activity of $[Cu^{II}\{H_x(tmdnTAA)\}]^{x+}$ complexes for the reduction of S^{IV} species in solution, several electrochemical experiments were conducted in anticipation to the mechanistic study of the catalyzed reduction of S^{IV} species.

Electrochemically Induced Reactions of S^{IV} Species with $[Cu^{II}\{H_x(tmdnTAA)\}]^{x+}$. The catalysis of the electrochemical reduction of S^{IV} species by monomeric $[Cu^{II}\{H_x(tmdnTAA)\}]^{x+}$ was investigated by cyclic voltammetry. A deaerated solution containing 0.01M $Et_4N \cdot ClO_4$, $1.0 \cdot 10^{-3}$ M $[Cu^{II}\{H_x(tmdnTAA)\}]^{x+}$ in 50% (*v*/*v*) DMF/H_2O and saturated with SO_2 was used to record the cyclic voltammogram. Another solution prepared without the complex was used as a blank. A discharge current developed in the voltammogram, which was larger in the solution containing the $[Cu^{II}\{H_x(tmdnTAA)\}]^{x+}$ complexes than in the blank, having a peak current i_{peak} at -0.72 V *vs.* the Ag/AgCl electrode. At variance with the catalyzed reduction of S^{IV}, the uncatalyzed reduction of S^{IV} was observed at -0.9 V *vs.* the Ag/AgCl electrode in the blank, with a much smaller value of i_{peak}. The augmented i_{peak} is indicative of the catalyzed reduction of the S^{IV} species. The catalyzed reaction occurred at a potential that is marginally more negative than the reduction potential of the couple $[Cu^{II}\{H_x(tmdnTAA)\}]^{x+}/[Cu^{I}\{H_x(tmdnTAA)\}]^{(x-1)+}$ (-0.70 V *vs.* Ag/AgCl), and should involve thence, the copper complexes in its mechanism. Both experimental observations, the increase in the discharge current, and the $+180$ mV shift of the potential when $[Cu^{II}\{H_x(tmdnTAA)\}]^{x+}$ complexes are present in the solution, are consistent with an EC′-type following reaction. This electrochemical process was defined by *Bard* and *Faulkner* as a special type of electrode reaction with a coupled homogeneous reaction [41b]. In the EC′ reaction sketched in *Scheme 2*, the reduced species R reacts with a species Z in solution to regenerate the oxidated state O [41b]. The conversion of Z to Y may evolve through the formation of a short-lived adduct, comprising the copper complexes and S^{IV} species. Pulse-radiolysis experiments, aimed to investigate the possible formation of such adducts, are described in a following section.

Cyclic voltammograms were also recorded with two solutions, pH 2 and 6, of $1.0 \cdot 10^{-3}$ M $[Cu^{II}\{H_x(tmdnTAA)\}]^{x+}$ in 50% (*v*/*v*) DMF/H_2O where $1.0 \cdot 10^{-3}$ M $(NH_4)_2SO_3$ was used instead of SO_2. A larger i_{peak} value resulted in the cyclic voltammogram

Scheme 2. *A Special Type of Electrochemical EC Reaction* (EC′) [41b], *Involving a Reaction of the Product R with a Nonelectroactive Species Z to Regenerate the Reactant O Reduced at the Electrode*

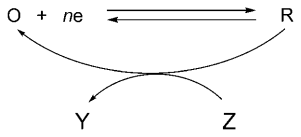

recorded at pH 2 than in the one at pH 6. In the solution with pH 2, the most abundant S^{IV} species was SO_2(aq). The distribution of species in *Table 1*, calculated on the basis of the equilibrium constants K_1 and K_2 (*Scheme 1*), shows a complete conversion of the $[Cu^{II}\{H_x(tmdnTAA)\}]^{x+}$ complexes to the $[Cu^{II}\{H_2(tmdnTAA)\}]^{2+}$ species at pH values lower than or equal to 5. The large i_{peak} value at pH 2 is indicative of a particular affinity between SO_2(aq) and the diprotonated species generated by the addition of one electron to $[Cu^{II}\{H_2(tmdnTAA)\}]^{2+}$.

Table 1. *Distribution of Cu^{II} Species and Rate Constants for Their Reactions with Pulse-Radiolytically Generated Radicals*

Radical[a])	pH	$[[Cu^{II}\{(tmdnTAA)\}]]$/ $[[Cu^{II}\{H(tmdnTAA)\}]^{+}]$	$[[Cu^{II}\{H(tmdnTAA)\}]^{+}]$/ $[[Cu^{II}\{H_2(tmdnTAA)\}]^{2+}]$	k [M^{-1} s^{-1}]
	2	$1:1.2\cdot10^{6}$	$4.5\cdot10^{-4}:1$	[b])
e^{-}_{aq}	5	$1:2.5\cdot10^{2}$	1 : 2.5	$4.3\cdot10^{10}$
$Me_2C^{\cdot}OH$				$2.0\cdot10^{9}$
e^{-}_{aq}	7	1 : 2.5	40 : 1	$1.5\cdot10^{10}$
$Me_2C^{\cdot}OH$				$2.2\cdot10^{8}$
$C^{\cdot}H_2OH$				$1.6\cdot10^{8}$
e^{-}_{aq}	10	$1.3\cdot10^{2}:1$	$1.3\cdot10^{4}:1$	$7.4\cdot10^{9}$

[a]) Reduction potentials of the radicals: e^{-}_{aq}, -2.75 V; $Me_2C^{\cdot}OH$, -1.20 V; $C^{\cdot}H_2OH$, -0.92 V; all potentials *vs.* NHE; values from [41c]. [b]) No pulse-radiolysis experiments were performed at pH 2.

In summary, the above-described experimental observations demonstrate that the monomeric Cu^{II} complex is able to catalyze the electrochemical reduction of S^{IV} species in homogeneous solution. Nevertheless, they are not capable of discerning the nature of the product of the catalyzed S^{IV} reduction. Hence, the product was investigated by the constant-potential electrolysis technique. The electrolyses were carried out in a three-electrode cell at -1.0 V *vs.* the Ag/AgCl electrode. To form a sufficiently large concentration of product, 50 ml of a deaerated solution, containing 0.03M HSO_3^- and $5\cdot10^{-3}$ M $[Cu^{II}\{H_x(tmdnTAA)\}]^{x+}$ in 50% (*v*/*v*) DMF/H_2O, was electrolyzed for 2 h delivering *ca.* 5 C to the electrode. In contrast to a nonelectrolyzed blank, the electrolyzed solution tested positive for $S_2O_4^{2-}$. Neither in the cyclic voltammetry nor in the controlled-potential electrolysis, the formation of Cu^0 was observed in the cathode.

Pulse Radiolysis. The electrochemical experiments suggested that the products of the $[Cu^{II}\{H_x(tmdnTAA)\}]^{x+}$ electrochemical reduction were capable of reacting with S^{IV} species before experiencing irreversible transformations to other products.

Pulse radiolysis was used to determine the fate of the $[Cu^{II}\{H_x(tmdnTAA)\}]^{x+}$ reduction products in the presence and absence of S^{IV} species. To this end, the reactions of the complex with $C^{\bullet}H_2OH$ and $Me_2C^{\bullet}OH$ radicals were investigated in aqueous solutions containing $1.0 \cdot 10^{-4}$ M to $4 \cdot 10^{-4}$ M of the Cu^{II} complex and 0.1M of MeOH or i-PrOH, and comparatively analyzed in the presence and absence of S^{IV} species. The solutions were deaerated and saturated with N_2O, and buffers of an adequate pH were used to keep the pH of the medium constant (pH 5 and 7) during and after the irradiation. The reaction of the e^-_{sol} with the complex was investigated with solutions of the same composition but deaerated and saturated with N_2.

The spectrum of the solutions changed when the pulse-radiolytically generated radicals ($R^{\bullet} = e^-_{sol}$, $C^{\bullet}H_2OH$, or $Me_2C^{\bullet}OH$) reacted with $[Cu^{II}\{H_x(tmdnTAA)\}]^{x+}$, $x = 1$ or 2. The observed spectroscopic changes when $R^{\bullet} = C^{\bullet}H_2OH$ or $Me_2C^{\bullet}OH$ are associated with the reduction of the Cu^{II} complex to $[Cu^{I}\{H_x(tmdnTAA)\}]^{(x-1)+}$ (*Eqn. 1*).

$$\begin{array}{ccc} [Cu^{II}\{H_2(tmdnTAA)\}]^{2+} + R^{\bullet} & \xrightarrow[-R^+]{} & [Cu^{I}\{H_2(tmdnTAA)\}]^{+} \\ -H^+ \downarrow\uparrow +H^+ & & -H^+ \downarrow\uparrow +H^+ \\ [Cu^{II}\{H(tmdnTAA)\}]^{+} + R^{\bullet} & \xrightarrow[-R^+]{} & [Cu^{I}\{H(tmdnTAA)\}] \end{array} \quad (1)$$

Typical time-resolved changes in the absorption spectrum caused by the reaction of $C^{\bullet}H_2OH$ radicals with the complex are shown in *Fig. 1*. The difference spectrum recorded with a delay of 10 μs from the irradiation is due to the mixture of Cu^{I} products in *Eqn. 1*. This assignment is based on the fact that the redox potential of the $C^{\bullet}H_2OH$ radical (*Table 1*) is too small for the reduction of the ligand, leaving the transfer of an electron from the radical to Cu^{II} as the only possible reaction (this reduction was observed at *ca.* -0.5 V *vs.* NHE (normal hydrogen electrode in cyclic voltammetry) [30–32]. Although the redox potentials of the e^-_{sol} and the $Me_2C^{\bullet}OH$ radicals are more negative than the one of the $C^{\bullet}H_2OH$ radical (*Table 1*), the spectra of the reaction products are identical to those observed when the tetraazaannulene complex is reduced by $C^{\bullet}H_2OH$ radicals. Because of the similarity of the spectroscopic changes, the same Cu^{I} products (*Eqn. 1*) must be formed in the reactions of e^-_{sol}, $C^{\bullet}H_2OH$, or $Me_2C^{\bullet}OH$ with the complex.

Due to the high concentration of complex relative to the concentrations of the radiolytically generated radicals, the process in *Eqn. 1* is kinetically pseudo-first-order with respect to radical concentration. Second-order rate constants were calculated from the slope of k_{psf} *vs.* $[Cu^{II}]_0$ plots, where k_{psf} is the pseudo-first-order rate constant of *Eqn. 1* and $[Cu^{II}]_0$ is the initial concentration of all the protonated forms of the complex in solution. The second-order rate constant k in *Table 1* shows a dependence on the solution's pH, which parallels the displacement of the equilibria in *Eqn. 1* with acid concentration. Moreover, there is a slight dependence of the rate constant on the redox potential of the radical. This dependence can be the result of the different redox potentials of the radicals (*Table 1*) which lead in turn to a radical-dependent driving force for *Eqn. 1*.

In addition to a decay of the absorbance at wavelengths of the band centered at 465 nm, a bleach of the solution showing a maximum change of the absorbance at *ca.*

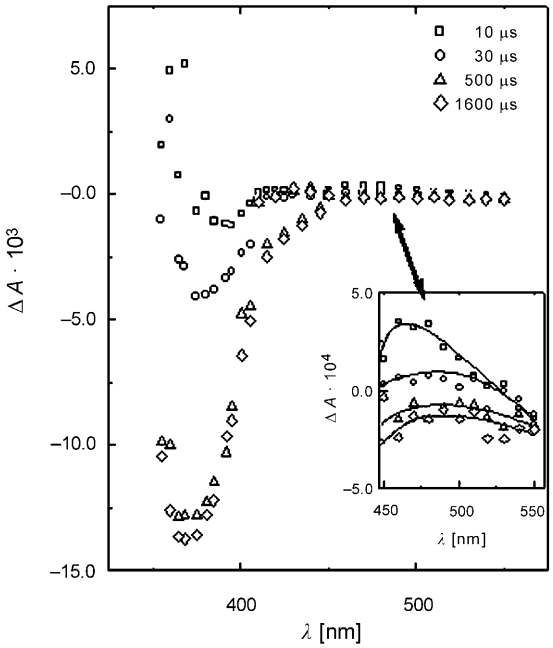

Fig. 1. *Time-resolved changes in the optical spectrum of a pulse-radiolyzed solution of [Cu^{II}{H$_x$(tmdnTAA)}]$^{x+}$ species.* The total concentration of Cu^{II} species, [Cu^{II}]$_0$, is 10^{-4} M, in N_2O-saturated 10% (*v*/*v*) MeOH/H_2O buffered at pH 5.2. The optical changes are caused after radiolytically generated C$^{\cdot}H_2OH$ radicals formed Cu^{I} species within the initial 10 μs. The subsequent bleach of the solution, λ_{max} 370 nm, is due to a reaction of the [Cu^{I}(ligand-radical)] complex produced from the Cu^{I} species.

370 nm was observed in a time period longer than 10 μs. These changes in the spectrum are related to the disproportionation of the [Cu^{I}{H$_x$(tmdnTAA)}]$^{(x-1)+}$ complexes into a [Cu^{I}(ligand-radical)] species, *i.e.*, [Cu^{I}{H$_x$(tmdnTAA)}$^{\cdot}$]$^{(2-x)-}$ (*Eqn. 2*).

$$2\,[\mathrm{Cu^{I}}\{\mathrm{H}_x(\mathrm{tmdnTAA})\}]^{(x-1)+}_{(x=1,2)} \rightarrow [\mathrm{Cu^{II}}\{\mathrm{H}_x(\mathrm{tmdnTAA})\}]^{x+} + [\mathrm{Cu^{I}}\{\mathrm{H}_x(\mathrm{tmdnTAA})\}^{\cdot}]^{(2-x)-} \qquad (2)$$

Linear plots of $(\Delta A_{inf} - \Delta A_0)/(\Delta A_{inf} - \Delta A_t)$ *vs.* time showed that the process is kinetically of second-order with respect to the concentration of [Cu^{I}{H$_x$(tmdnTAA)}]$^{(x-1)+}$ (ΔA_i is the absorbance change measured at the end of the reaction ($i = \mathrm{inf}$), at the beginning of the reaction ($i = 0$), and at time t($i = t$)). Moreover, the half-life period of the reaction ($t_{1/2}$)[1]) was determined as proportional to

[1]) The half-life periods ($t_{1/2}$) were obtained by fitting the oscillographic traces (λ_{ob} 370 nm) over the first half-life period to the function $A\ (1 - e^{-1.44t/t_{1/2}})$. Series expansions of the function and the integrated rate law for the competitive formation of the adduct, *Eqns. 2–5*, are identical to the sixth polynomial degree.

the initial concentration of all the protonated forms, $[Cu^{II}]_0$. Attending the kinetics of the reaction, the changes in the spectrum can be explained in terms of the transformation of a [Cu^{I}(ligand-radical)] complex, *i.e.*, of $[Cu^{I}\{H_x(tmdnTAA)\}^{\bullet}]^{(2-x)-}$, produced by the disproportionation of the $[Cu^{I}\{H_x(tmdnTAA)\}]^{(x-1)+}$ species (*Eqn. 3*). A steady-state treatment on the concentration of the $[Cu^{I}\{H_x(tmdnTAA)\}^{\bullet}]^{(2-x)-}$ species with the rate equations of *Eqns. 2* and *3* gives the rate law of *Eqn. 4* for the decay of Cu^{I}, where $[[Cu^{I}\{H_x(tmdnTAA)\}]^{(x-1)+}]_T = [[Cu^{I}\{H_2(tmdnTAA)\}]^{+}] + [[Cu^{I}\{H(tmdnTAA)\}]]$.

$$[Cu^{I}\{H_x(tmdnTAA)\}^{\bullet}]^{(2-x)-} + 2\,H^{+} \xrightarrow{k_3} \text{product} \tag{3}$$

$$-\frac{d\,[[Cu^{I}\{H_x(tmdnTAA)\}]^{(x-1)+}]_T}{dt} = k_o[[Cu^{I}\{H_x(tmdnTAA)\}]^{(x-1)+}]_T^2$$

$$\left(k_o = k_3 K \frac{1}{[Cu^{II}]_0 + k_3/k_b}\right) \tag{4}$$

To account for the proportionality of $t_{1/2}$ to $[Cu^{II}]_0$, one must assume that $[Cu^{II}]_0 > k_3/k_b$. Under this condition, the expression of the overall rate constant, k_o, is reduced to $k_o = k_3\,k_f/k_b$. A ratio of the overall rate constant k_o to the extinction coefficient (ε), *i.e.*, $k_o/\varepsilon = k_3\,k_f/\varepsilon\,k_b \approx 1.8 \cdot 10^3$ cm s^{-1}, was calculated from oscillographic traces recorded at λ_{ob} 465 nm.

The participation of $[Cu^{I}\{H_x(tmdnTAA)\}^{\bullet}]^{(2-x)-}$ in the reaction mechanism (*Eqns. 1–3*) is consistent with the kinetics of the process. Its presence in very small concentrations is expected on the basis of the rapid conversion to products (*Eqn. 3*) and the small equilibrium constant, K_f, calculated with the reduction potentials of the couples $[Cu^{II}\{H_x(tmdnTAA)\}]^{x+}/[Cu^{I}\{H_x(tmdnTAA)\}]^{(x-1)+}$, $\varepsilon^0 \approx -0.5$ V *vs.* NHE in DMF, and $[Cu^{I}\{H_x(tmdnTAA)\}]^{(x-1)+}/[Cu^{I}\{H_x(tmdnTAA\}^{\bullet})]^{(2-x)-}$, $\varepsilon^0 \approx -0.8$ V *vs.* NHE in DMF [30].

On the basis of the known reactions of macrocyclic complexes [30], two processes can account for the decay of the $[Cu^{I}\{H_x(tmdnTAA)\}^{\bullet}]^{(2-x)-}$ species (*Eqn. 3*) and the spectroscopic changes associated with the decay of $[Cu^{I}\{H_x(tmdnTAA)\}]^{(x-1)+}$ (*Fig. 1*). One process consists in the conversion of the macrocycle ligand into an easily hydrolyzable open-cycle ligand which liberates Cu^{+}_{aq} and/or Cu^{2+}_{aq} ions. The other process is the hydrogenation of a double bond in the macrocycle reducing the electronic delocalization in the tetraazaannulene macrocycle. A consequence of the macrocycle opening or hydrogenation is the disappearance of the intense ligand-centered electronic transitions located at $\lambda_{max} < 400$ nm in the spectrum of $[Cu^{II}\{H_x(tmdnTAA)\}]^{x+}$[30]. The possible products of the macrocycle hydrolysis, Cu^{I}_{aq} and Cu^{II}_{aq}, were investigated in the irradiated solutions to establish which one of these processes is associated with *Eqn. 3*. Solutions with the composition indicated above were irradiated with a train of *ca.* 100 radiolytic pulses to accrete enough reaction product. The irradiation resulted in a *ca.* 10% conversion of the initial concentration of complex to products. Neither Cu^{I}_{aq} nor Cu^{II}_{aq} were detected in samples

of the irradiated solution. Considering the detection limit of the analytical method, it was estimated that 90% or more of the product formed after the reduction of $[Cu^{II}\{H_x(tmdnTAA)\}]^{x+}$ has a closed-ring macrocycle where a double bond in the ligand has been converted to a single bond by the addition of two H-atoms, *e.g.*, as in the species $[Cu^{II}\{H_x(tmdnTAAH_2)\}]^{x+}$.

Adducts Formed between S^{IV} Species and $[Cu^{I}\{H_x(tmdnTAA)\}]^{(x-1)+}$ Species. The reduction of the $[Cu^{II}\{H_x(tmdnTAA)\}]^{x+}$ complexes by pulse-radiolytically generated radicals was also conducted in the presence of S^{IV} anions ($[SO_3^{2-}]_T = [HSO_3^-] + [SO_3^{2-}]$) under similar conditions, to investigate their possible interactions. No reactions of the $C^{\cdot}H_2OH$ radicals with the S^{IV} species occurred with the concentrations used in these experiments. The influence of the S^{IV} on the radical-induced change in the solutions spectrum is shown in *Fig. 2*. In summary, the presence of S^{IV} species suppresses the bleach of the 370 nm absorbance in the solution spectrum (see *Fig. 1*), and a new absorption band appears at λ_{max} *ca.* 360 nm. Relative to *Fig. 1*, the absorbance between 450 and 530 nm, where $[Cu^{I}\{H_x(tmdnTAA)\}]^{(x-1)+}$ species have more intense absorption bands than the other species, is augmented. The broad absorption band with λ_{max} *ca.* 360 nm reveals the formation of new transient species in addition to those previously described (*Eqns. 2* and *3*). To quantify its presence, the absorbance change, ΔA, was measured at 350 nm as a function of $[SO_3^{2-}]_T$. The augmented absorbance between 450 and 530 nm is due to the lower consumption of $[Cu^{I}\{H_x(tmdnTAA)\}]^{(x-1)+}$

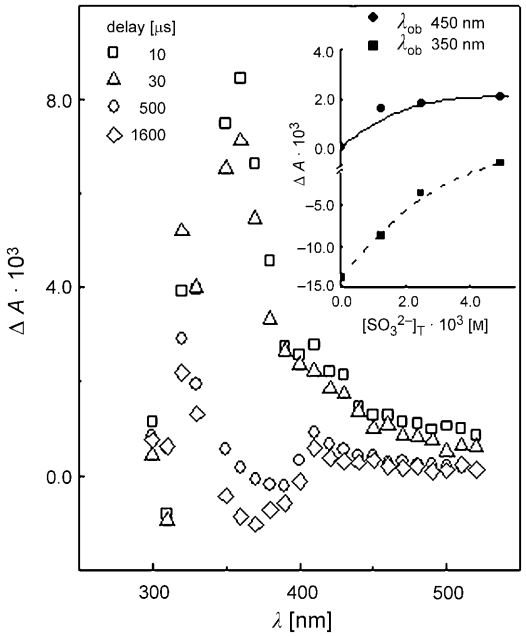

Fig. 2. *Time-resolved changes in the absorption spectrum of a pulse-radiolyzed solution containing 0.1*M *MeOH, 10^{-4}* M *$[Cu^{II}]_0$, and $4.0 \cdot 10^{-3}$* M *$[SO_3^{2-}]_T$ in N_2O-saturated H_2O at pH 5.2.* A key for the delays from the radiolytic pulse is given in the figure. The inset shows the dependence of the absorbance change with $[SO_3^{2-}]_T$.

via Eqns. 2 and *3*. To see how S^{IV} species prevented the transformation of the Cu^{I} complexes, ΔA was also measured at 450 nm with 100 to 190 μs delays from the radiolytic pulse. The monotonic increase of ΔA with $[SO_3^{2-}]_T$ at 450 nm and 350 nm can be seen in the inset of *Fig. 2*. It shows that $[Cu^{I}\{H_x(tmdnTAA)\}]^{(x-1)+}$ species become more stable and that the concentration of the transient species absorbing with λ_{max} *ca.* 360 nm increases with $[SO_3^{2-}]_T$. In this way, the spectroscopic evidence points to the formation of an adduct $[Cu^{I}\{H_x(tmdnTAA)\}(SO_2)]^{(x-1)+}$ involving these species and to a lesser decay of the Cu^{I} species *via Eqns. 2* and *3*.

Kinetics of the EC′ Reaction. The kinetics of the $[Cu^{I}\{H_x(tmdnTAA)\}(SO_2)]^{(x-1)+}$ formation was investigated at 370 nm as a function of $[SO_3^{2-}]_T$. The reciprocal of the half-life period $t_{1/2}$ [58] of the recovery process increased with total sulfite concentration depending also on proton concentration (*Fig. 3* and *Table 2*) as it is expected when *Eqns. 2* and *3* are coupled to *Eqns. 5* and *6*.

$$SO_2(aq) \rightleftharpoons HSO_3^- + H^+ \tag{5}$$

$$[Cu^{I}\{H_x(tmdnTAA)\}]^{(x-1)+} \xrightarrow{+SO_2(aq)} [Cu^{I}\{H_x(tmdnTAA)\}SO_2]^{(x-1)+} \tag{6}$$

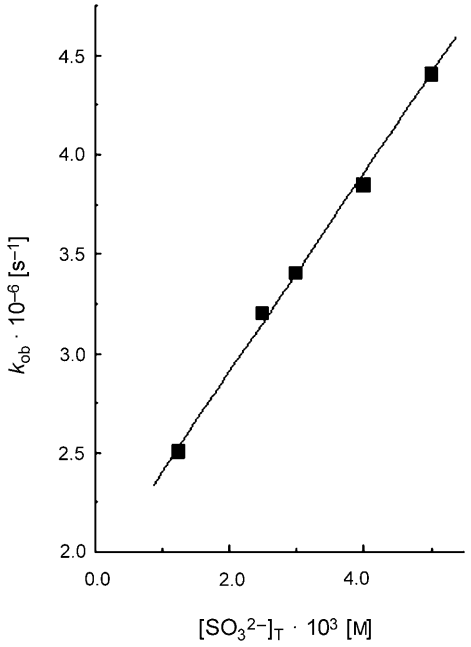

Fig. 3. *Dependence of the rate constant* (k_{ob}) *for the suppression of the 370 nm bleach on the total sulfite-ion concentration.* The reaction kinetics was investigated by pulse radiolysis with solutions containing 0.1M MeOH, 10^{-4} M $[Cu^{II}]_0$ and a variable concentration of $[SO_3^{2-}]_T$ in N_2O-saturated H_2O at pH 5.2.

On the other hand, the decay of $[Cu^{I}\{H_x(tmdnTAA)\}(SO_2)]^{(x-1)+}$ was followed at 450 nm in a time period longer than 200 μs to avoid complications from the bleach of the solution at shorter wavelengths. Linear plots of ΔA^{-1} *vs.* time demonstrated that the process is kinetically second-order with respect to the $[Cu^{I}\{H_x(tmdnTAA)\}(SO_2)]^{(x-1)+}$ concentration. Values for the ratio of the rate constant k to the 450 nm extinction coefficient ε (*Table 2*) are independent of $[SO_3^{2-}]_T$ and show a dependence on the solution's pH. *Eqn. 7*, and/or *Eqns. 8* and *9*, account for a decay of $[Cu^{I}\{H_x(tmdnTAA)\}(SO_2)]^{(x-1)+}$ that reforms the parent $[Cu^{II}\{H_x(tmdnTAA)\}]^{x+}$ complexes. Restoration of the latter suppresses the bleaching of the solution in the 360 nm region of the spectrum as it can be seen from a comparison of *Figs. 1* and *2*. Furthermore, the $[Cu^{II}\{H_x(tmdnTAA)\}]^{x+}$ catalysis of the electrochemical reduction of S^{IV} species can be rationalized with *Eqns. 6–9*. The pulse-radiolysis results suggest that $[Cu^{II}\{H_x(tmdnTAA)\}]^{x+}$ can be reduced in the electrode and the Cu^{I} products react according to *Eqns. 7–9*.

Table 2. *Reciprocal of the Half-Life Period* ($1/t_{1/2}$) *for the Formation of* $[Cu^{I}\{H_x(tmdnTAA)\}(SO_2)]^{(x-1)+}$ *and the Ratio of the Second-Order Rate Constant to the 450 nm Extinction Coefficient* (k/ε) *for the Decay of the Same Species*

$[SO_3^{2-}]_T$ [M]	pH	$1/t_{1/2}$ [s^{-1}]	k/ε [cm s^{-1}]
$5.0 \cdot 10^{-3}$	9.5	$4.4 \cdot 10^3$	$4.5 \cdot 10^6$
$4.0 \cdot 10^{-3}$	9.5	$3.9 \cdot 10^3$	$4.2 \cdot 10^6$
$2.5 \cdot 10^{-3}$	9.5	$3.1 \cdot 10^3$	$3.7 \cdot 10^6$
$1.25 \cdot 10^{-3}$	9.5	$2.5 \cdot 10^3$	$4.1 \cdot 10^6$
$5.0 \cdot 10^{-3}$	7	$5.0 \cdot 10^3$	$9.6 \cdot 10^6$
$5.0 \cdot 10^{-3}$	5.2	$7.0 \cdot 10^4$	$1.8 \cdot 10^7$

$$2\,[Cu^{I}\{H_x(tmdnTAA)\}(SO_2)]^{(x-1)+} \rightarrow 2\,[Cu^{II}\{H_x(tmdnTAA)\}]^{x+} + S_2O_4^{2-} \quad (7)$$

$$[Cu^{I}\{H_x(tmdnTAA)\}(SO_3)]^{x-3} + 2\,H^+ \rightarrow [Cu^{II}\{H_x(tmdnTAA)\}]^{x+} + SO_2^{\cdot-} + H_2O \quad (8)$$

$$SO_2^{\cdot-} \rightleftharpoons S_2O_4^{2-} \quad (9)$$

Theoretical Considerations on the S^{IV}-Containing Intermediates. Having demonstrated that the $[Cu^{II}\{H_x(tmdnTAA)\}]^{x+}$-catalyzed S^{IV} reduction occurs through a EC′ mechanism (*Scheme 2*), we were interested in discerning the nature of the transient states, which are associated with the absorption at λ_{max} *ca.* 360 nm and with S^{IV} coordinated to $[Cu^{I}\{H_x(tmdnTAA)\}]^{(x-1)}$. To this end, we applied theoretical methodologies to compare the structural and electronic characteristics of the species that can be formed as reaction intermediates.

The structures, atomic charges (*cf. Table 3*), and energies of $[Cu^{I}\{H_x(tmdnTAA)\}]^{(x-1)+}$ ($x = 0$, 1 and 2), and of the possible transient species formed in the presence of SO_2 and hydrogen sulfite ions, were investigated after

optimization of the geometries at the DFT/LANL2DZ level. As ambidentate ligands, *S*-oxides can coordinate to Cu-ions through the S- or O-atoms. Attending to this possibility, the nature of the transients was analyzed by the comparison of S- and O-coordination modes of HSO_3^- and SO_2 species to the metal center of the $[Cu^I\{H_x(tmdnTAA)\}]^{(x-1)+}$ ($x = 0, 1$ and 2) complexes. Neither species with coordinated HSO_3^- nor with an additional H_2O molecule forming octahedral compounds were stabilized.

Table 3. *Calculated Electronic Charges of the Cu-Center and the Atoms Coordinated to the Metal Center of Tetraazaannulene Complexes Participating in Redox Reactions*

	x	Cu	N	S	O(1)[a])	O(2)
$[Cu^I\{H_x(tmdnTAA)\}]^{x+}$	0	+0.6	−0.8			
	1	+0.46	−0.74 −0.64 −0.60, −0.12			
	2	+0.39	−0.60, −0.19			
SO_2				0.84	−(0.42 ± 0.005)[b])	
$[Cu^I\{H_x(tmdnTAA)\}OSO]^{x+}$	1	+0.57	−0.67, −0.52, −0.43, −0.17	0.59	−(0.55 ± 0.03)[b])	
	2	+0.52	−0.55, −0.41, −0.40, −0.30	0.74	−(0.55 ± 0.03)[b])	

[a]) O of SO_2 bonded to the Cu-center. [b]) Average charge when differences between charges are equal to or less than 5%.

We mainly focused on the evaluation of the TDDFT (time-dependent density functional theory) calculated UV/VIS spectra and its comparison with experiment, as the evaluation of the free energy of binding is somehow hampered by the low stability of the short-lived transient intermediates. Nevertheless, the analysis of the molecular-orbital interactions helped to justify the relative stability calculated for the $[Cu^I\{H(tmdnTAA)\}]$ species.

In the nonprotonated $[Cu^I(tmdnTAA)]^-$ complex, the Cu-ion is coordinated to the imine N-atoms defining a square-planar symmetry in the first coordination shell (*Fig. 4*,*a*). The CuN_4 polyhedron is in an ideal planar arrangement that optimizes electron delocalization and stabilizes the Cu−N binding (*Fig. 5*). The naphtho moieties are bent out of the plane decreasing the symmetry of the complex to C_{2v}. The coordination of SO_2 to the nonprotonated complex does not converge to a stable structure after geometry optimization, in agreement with a nonfavorable change in the coordination number of Cu^I from 4 to 5 that would result from binding.

The symmetry is lowered by single and double protonation of the N-atoms, as the Cu−N bonds involving the amine N-atom are elongated (see *Fig. 4*,*b* and *c*, and *Table 4*). N-Protonation disrupts the electron delocalization in the immediate copper coordination sphere, localizing the electron density on the metal center and on C(2) (=C(β)) of the prop-1-en-1-yl-3-ylidene moiety (*Scheme 1*), farther from the amine N-atom (*Fig. 6*).

We were able to identify S- and O-coordinated $[Cu^I\{H_x(tmdnTAA)\}]^{(x-1)+}$ ($x = 1$ and 2) structures as minima on the potential hypersurface. However, none of the S-coordinated adducts is stable relative to the separated species, representing, hence, relative minima. On the other hand, O-coordination is slightly favored (2 kcal/mol, *Table 4*) in the single-protonated complex relative to the diprotonated one. The

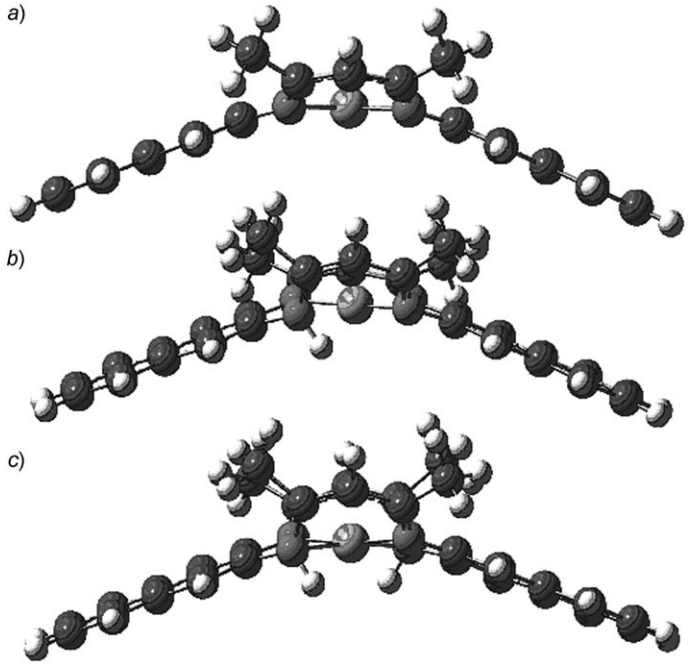

Fig. 4. *Calculated structures of* $[Cu^{I}\{H_x(tmdnTAA)\}]^{(x-1)+}$: a) x = *0*, b) x = *1 and* c) x = *2*

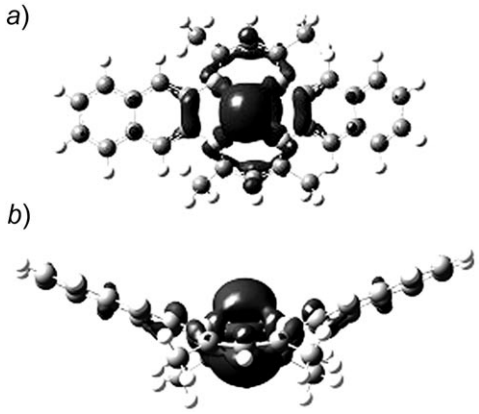

Fig. 5. a) *Top and* b) *lateral views of the HOMO-1 orbital of the* $[Cu^{I}(tmdnTAA)]^{-}$ *species* ($x = 0$)

analysis of the molecular orbitals shows that the first one implies a side-on coordination stabilized by the simultaneous interaction of an antibonding S=O π orbital with the Cu-atom and C(β) in the prop-1-en-1-yl-3-ylidene moiety of the macrocycle, far from the H-atom bearing the amine N-atom (*Fig. 7*). A second protonation decreases the electron density of the macrocycle destabilizing the binding. The structural character-

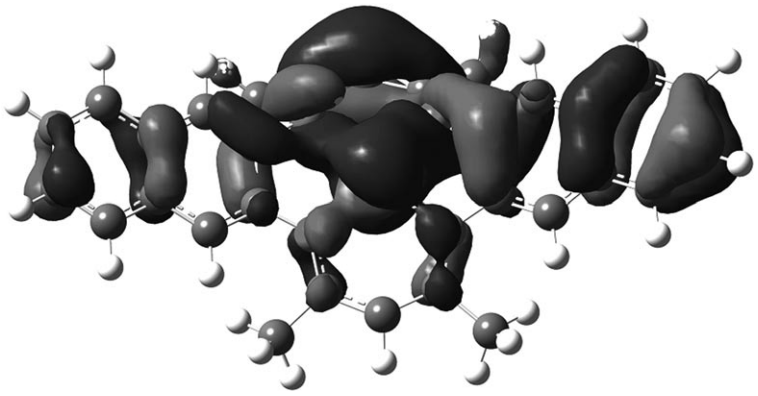

Fig. 6. *Surface representation of the HOMO-1orbital in the [Cu^{I}{H(tmdnTAA)}] species*

Table 4. *Calculated Bond Distances in the Cu Coordination Sphere, Energies of Tetraazaannulene Complexes Participating in Redox Reactions* (see *Fig. 8*) *and Their Cu^{I}-to-SO$_2$ Charge-Transfer Spectroscopic Features*

	x	Cu–N [Å]	Cu–O [Å]	ΔG[a]) [kcal/mol]	λ[b]) [nm]
$[Cu^{I}\{H_x(tmdnTAA)\}]^{(x-1)+}$	0	2.012			
	1	2.218, 1.944, 1.965, 2.010			
	2	2.181[c]), 1.961[c])			
$[Cu^{I}\{H_x(tmdnTAA)\}(SO_2)]^{(x-1)+}$	1	2.083[c]), 2.400[c])	2.100	3.6	355 (0.35)
	2	2.255[c]), 2.605[c])	1.979	2.1	396 (0.60)

[a]) Binding energy of SO_2 to the metal center, calculated as the free-energy difference between the bonded species and the separated ones, corrected for BSSE and solvent effects (negative values indicate that a given coordination of SO_2 is not stable relative to the separated species). [b]) Calculated wavelength for the $Cu^{I} \rightarrow SO_2$ charge-transfer transition. Intensities are given in parentheses. [c]) Average of two bond distances when differences between them is less than $5 \cdot 10^{-3}$ Å.

istics of the stable adducts are shown in *Fig. 8*. In the interactions described previously, the SO_2 S-atom is acting as a *Lewis* acid, accepting electron density from the macrocycle. This coordination scheme is not effective in the case of S-binding to the Cu-center, as the electron density of the $[Cu^{I}\{H_x(tmdnTAA)\}]^{(x-1)+}$ ($x = 1$ and 2) complexes is mainly localized at C(β) of the prop-1-en-1-yl-3-ylidene moiety.

The TDDFT calculations associate a band at 360 nm with a metal-to-ligand charge-transfer transition in the $[Cu^{I}\{H(tmdnTAA)\}](SO_2)$ species, from orbitals centered in the ligand and delocalized on the macrocycle to antibonding SO_2 orbitals. A similar band is calculated for the diprotonated adduct, red shifted to 396 nm. The shift to lower energy can be explained by the diminished delocalization in the macrocycle of the Cu-orbital associated with the transfer.

The calculated bands are shown in *Table 4*. In all the cases, some d–π mixing increases their intensity. Additional bands (not shown), calculated in the 400–450 nm region, are associated with d–$\pi \rightarrow \pi$ transitions in the macrocycle. It is possible,

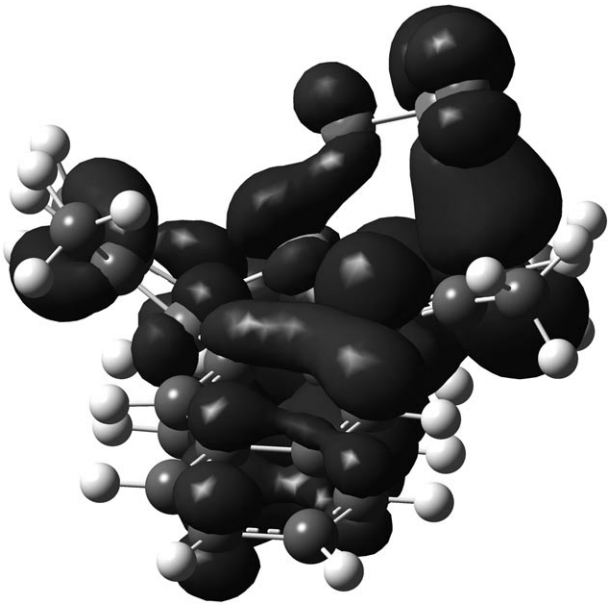

Fig. 7. *Surface representation of the bonding interactions* (HOMO-1 orbital) *in the [Cu{H(tmdn-TAA)}(SO_2)] species*

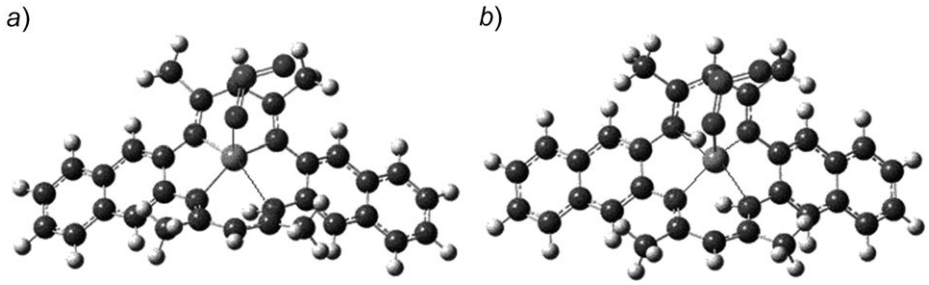

Fig. 8. *Calculated structures of [Cu^I{H_x(tmdnTAA)}(SO_2)]$^{(x-1)+}$ species:* a) x = *1 and* b) x = *2*

therefore, to account for the spectroscopic changes shown in *Fig. 2* with the mentioned electronic transitions and distribution of intensities in the spectrum of the [Cu^I{H_x(tmdnTAA)}(SO_2)]$^{(x-1)+}$ species. For the pH value close to 5, at which the spectrum shown in *Fig. 2* was determined, the monoprotonation of the macrocycle is favored, and O-coordinated species can be formed, giving rise to the peaks close to 360 nm. The peaks close to 400 nm can be assigned to the presence of a lower concentration of O-coordinated diprotonated species in equilibrium.

Conclusions. – By means of radiolytic experiments and assisted by theoretical calculations, we established the formation of adducts between SO_2 and [Cu^I{H_x(tmdnTAA)}]$^{(x-1)+}$ in the mechanism of the radiolytically initiated reduction

of S^{IV} species. Since the reduction of $[Cu^{II}\{H_x(tmdnTAA)\}]^{x+}$ at the GCE produces $[Cu^{I}\{H_x(tmdnTAA)\}]^{(x-1)+}$ species, it can be expected that similar adducts between SO_2 and $[Cu^{I}\{H_x(tmdnTAA)\}]^{(x-1)+}$ are formed when the electrochemical reduction of S^{IV} species is catalyzed by the $[Cu^{II}(tetraazaannulene)]$ complexes. These inner-sphere pathways for the reduction of the S^{IV} species parallel those observed when the $[Cu^{II}(tetraazaannulene)]$ and $[Ni^{II}(tetraazaannulene)]$ complexes catalyzed the reduction of CO_2 [30]. It must be noted, however, that in the adducts of SO_2 with Cu^{I}, the metal center functions as an electrophile and favors the O-coordination, whereas it coordinates to C in the CO_2 adducts. In terms of new catalysts for the reduction of SO_2 and/or CO_2 in homogeneous solution, oligomers of the tetraazaannulene complexes merit attention because of the established high catalytic efficiency of the tetraazaannulene polymers deposited on an electrode surface [31]. They appear to be more efficient catalysts than the monomeric complexes in homogeneous solution. Among the oligomers with a good solubility in various solvents, only dimers of the tetraazaannulene complexes have been isolated and characterized [58]. It is possible that larger oligomers, having also good solubility in solvents appropriate for the reduction of SO_2, will be more efficient catalysts of the S^{IV} reduction in homogeneous solution. The preparation of such polymers by means of radical-initiated oligomerization processes as well as their application to the catalysis of reactions in homogeneous solution are subjects of a present research [59].

The work described herein was supported by the *Office of Basic Energy Sciences of the US Department of Energy*. This is contribution No. NDRL-4785 from the Notre Dame Radiation Laboratory. *M. V.*, *J. Z.*, and *J. C.* acknowledge support from the *Comisión National de Investigación Cientifica y Technológica* (*CONICYT*; #1060030). Generous allocation of computing resources by the Center for Research Computing, University of Notre Dame, is also gratefully acknowledged.

REFERENCES

[1] M. P. Donzello, C. Ercolani, K. M. Kadish, G. Ricciardi, A. Rosa, P. A. Stuzhin, *Inorg. Chem.* **2007**, *46*, 4145.
[2] Q. Zeng, M. Li, D. Wu, C. Liu, S. Lei, S. An, C. Wang, *Cryst. Growth Des.* **2007**, *7*, 1497.
[3] N. McCann, G. A. Lawrance, Y.-M. Neuhold, M. Maeder, *Inorg. Chem.* **2007**, *46*, 4002.
[4] F. Cuenot, M. Meyer, E. Espinosa, R. Guilard, *Inorg. Chem.* **2005**, *44*, 7895; M. Meyer, L. Frémond, E. Espinosa, R. Guilard, Z. Ou, K. M. Kadish, *Inorg. Chem.* **2004**, *43*, 5572.
[5] M.-S. Liao, J. D. Watts, M.-J. Huang, *J. Phys. Chem., A* **2005**, *109*, 7988.
[6] A. N. Vedernikov, M. Pink, K. G. Caulton, *Inorg. Chem.* **2004**, *43*, 4300.
[7] D. B. Rorabacher, *Chem. Rev.* **2004**, *104*, 651.
[8] L. M. Mirica, X. Ottenwaelder, T. D. P. Stack, *Chem. Rev.* **2004**, *104*, 1013.
[9] E. A. Lewis, W. B. Tolman, *Chem. Rev.* **2004**, *104*, 1047.
[10] G. Chaka, J. L. Sonnenberg, H. B. Schlegel, M. J. Heeg, G. Jaeger, T. J. Nelson, L. A. Ochrymowycz, D. B. Rorabacher, *J. Am. Chem. Soc.* **2007**, *129*, 5217.
[11] J. W. Sibert, P. B. Forshee, G. R. Hundt, A. L. Sargent, S. G. Bott, V. Lynch, *Inorg. Chem.* **2007**, *46*, 10913.
[12] C. P. Kulatilleke, *Polyhedron* **2007**, *26*, 1166.
[13] G. Gasser, M. J. Belousoff, A. M. Bond, Z. Kosowski, L. Spiccia, *Inorg. Chem.* **2007**, *46*, 1665.
[14] W. L. Man, W. W. Y. Lam, W. Y. Wong, T. C. Lau, *J. Am. Chem. Soc.* **2006**, *128*, 14669.
[15] E. I. Solomon, U. M. Sundaram, T. E. Machonkin, *Chem. Rev.* **1996**, *96*, 2563.
[16] G. McRobbie, G. C. Valks, C. J. Empson, A. Khan, J. D. Silversides, C. Pannecouque, E. De Clercq, S. G. Fiddy, A. J. Bridgeman, N. A. Young, S. J. Archibald, *Dalton Trans.* **2007**, 5008.

[17] M. M. Rosenkilde, L. O. Gerlach, S. Hatse, R. T. Skerlj, D. Schols, G. J. Bridger, T. W. Schwartz, *J. Biol. Chem.* **2007**, *282*, 27354.
[18] T. Hunter, I. J. McNae, X. Liang, J. Bella, S. Parsons, M. D. Walkinshaw, *Proc. Natl. Acad. Sci. U.S.A.* **2005**, *102*, 2288.
[19] R. H. Holm, P. Kennepohl, E. I. Solomon, *Chem. Rev.* **1996**, *96*, 2239.
[20] P. Antunes, R. Delgado, M. G. B. Drew, V. Felix, H. Maecke, *Inorg. Chem.* **2007**, *46*, 3144.
[21] E. I. Solomon, *Inorg. Chem.* **2006**, *45*, 8012.
[22] T. Haltia, K. Brown, M. Tegoni, C. Cambillau, M. Saraste, K. Mattila, K. Djinovic-Carugo, *Biochem. J.* **2003**, *369*, 77.
[23] S. Ghosh, S. I. Gorelsky, P. Chen, I. Cabrito, J. J. G. Moura, I. Moura, E. I. Solomon, *J. Am. Chem. Soc.* **2003**, *125*, 15708.
[24] J. M. Chan, J. A. Bollinger, C. L. Grewell, D. M. Dooley, *J. Am. Chem. Soc.* **2004**, *126*, 3030.
[25] S. I. Gorelsky, S. Ghosh, E. I. Solomon, *J. Am. Chem. Soc.* **2006**, *128*, 278.
[26] M. Calligaris, O. Carugo, *Coord. Chem. Rev.* **1996**, *153*, 83.
[27] R. G. M. Moreno, M. V. Alipázaga, O. F. Gomes, E. Linares, M. H. G. Medeiros, N. Coichev, *J. Inorg. Biochem.* **2007**, *101*, 866.
[28] S. C. Gibney, G. Ferraudi, M. Shang, *Inorg. Chem.* **1999**, *38*, 2898 and refs. cit. therein.
[29] V. Lepentsiotis, J. Domagala, I. Grgic, R. van Eldik, J. G. Muller, C. J. Burrows, *Inorg. Chem.* **1999**, *38*, 3500.
[30] J. Costamagna, G. Ferraudi, J. Canales, J. Vargas, *Coord. Chem. Rev.* **1996**, *148*, 221.
[31] J. P. Muena, M. Villagrán, J. Costamagna, M. J. Aguirre, *J. Coord. Chem.* **2008**, *61*, 479.
[32] J. Costamagna, G. Ferraudi, M. Villagran, E. Wolcan, *J. Chem. Soc., Dalton Trans.* **2000**, 2631.
[33] R. Escudero, M. Villagran, J. Costamagna, G. Ferraudi, *J. Coord. Chem.* **2003**, *56*, 1233.
[34] F. Armijo, G. Ferraudi, F. Isaacs, M. J. Aguirre, J. Costamagna, *Inorg. Chim. Acta* **2006**, *359*, 2281.
[35] S. K. Dutta, G. Ferraudi, *J. Phys. Chem., A* **2001**, *105*, 4241.
[36] S. Thomas, G. T. Ruiz, G. Ferraudi, *Macromolecules* **2006**, *39*, 6615.
[37] G. L. Hug, Y. Wang, C. Schöneich, P.-Y. Jiang, R. W. Fesenden, *Radiat. Phys. Chem.* **1999**, *54*, 559.
[38] G. V. Buxton, C. L. Greenstock, W. P. Hellman, A. B. Ross, W. Tsang, *J. Phys. Chem. Ref. Data* **1988**, *17*, 513.
[39] N. Getoff, A. Ritter, F. Schworer, *Radiat. Phys. Chem.* **1993**, *41*, 797.
[40] C. Barrera, I. Zhukov, E. Villagran, F. Bedioui, M. A. Paez, J. Costamagna, J. H. Zagal, *J. Electroanal. Chem.* **2006**, *589*, 212.
[41] a) A. J. Bard, L. R. Faulkner, in 'Electrochemical Methods, Fundamentals, and Applications', Chapt. 1 and 3, John Wiley & Sons, 1980; b) A. J. Bard, L. R. Faulkner, in 'Electrochemical Methods, Fundamentals, and Applications', John Wiley & Sons, 1980, p. 430; c) P. Wardman, *J. Phys. Chem. Ref. Data* **1989**, *18*, 1637
[42] E. M. Kosower, J. L. Cotter, *J. Am. Chem. Soc.* **1964**, *86*, 5524, and refs. cit. therein.
[43] M. J. Frisch, G. W. Trucks, H. B. Schlegel, G. E. Scuseria, M. A. Robb, J. R. Cheeseman, J. A. Montgomery Jr., T. Vreven, K. N. Kudin, J. C. Burant, J. M. Millam, S. S. Iyengar, J. Tomasi, V. Barone, B. Mennucci, M. Cossi, G. Scalmani, N. Rega, G. A. Petersson, H. Nakatsuji, M. Hada, M. Ehara, K. Toyota, R. Fukuda, J. Hasegawa, M. Ishida, T. Nakajima, Y. Honda, O. Kitao, H. Nakai, M. Klene, X. Li, J. E. Knox, H. P. Hratchian, J. B. Cross, V. Bakken, C. Adamo, J. Jaramillo, R. Gomperts, R. E. Stratmann, O. Yazyev, A. J. Austin, R. Cammi, C. Pomelli, J. W. Ochterski, P. Y. Ayala, K. Morokuma, G. A. Voth, P. Salvador, J. J. Dannenberg, V. G. Zakrzewski, S. Dapprich, A. D. Daniels, M. C. Strain, O. Farkas, D. K. Malick, A. D. Rabuck, K. Raghavachari, J. B. Foresman, J. V. Ortiz, Q. Cui, A. G. Baboul, S. Clifford, J. Cioslowski, B. B. Stefanov, G. Liu, A. Liashenko, P. Piskorz, I. Komaromi, R. L. Martin, D. J. Fox, T. Keith, M. A. Al-Laham, C. Y. Peng, A. Nanayakkara, M. Challacombe, P. M. W. Gill, B. Johnson, W. Chen, M. W. Wong, C. Gonzalez, J. A. Pople, Gaussian 03, Revision C.02, Gaussian, Inc., Pittsbourgh, PA, 2003.
[44] D. L. Harris, *Curr. Opin. Chem. Biol.* **2001**, *5*, 724.
[45] L. Noodleman, T. Lovell, W.-G. Li, J. Han, F. Himo, *Chem. Rev.* **2004**, *104*, 459.
[46] E. I. Solomon, R. K. Szilagyi, G. S. DeBeer, L. Basumallick, *Chem. Rev.* **2004**, *104*, 419.
[47] G. E. Estiu, K. Merz, *J. Phys. Chem.* **2007**, *111*, 10263.

[48] G. E. Estiu, D. Suarez, K. Merz, *J. Comput. Chem.* **2006**, *27*, 1240.
[49] A. D. Becke, D. R. Yarkony, in 'Modern Electronic Structure Theory', Part II, World Scientific, Singapore, 1995.
[50] W. J. Hehre, L. Radom, P. v. R. Schleyer, J. A. Pople, 'Ab Initio Molecular Orbital Theory', John Wiley & Sons, New York, 1986.
[51] P. J. Hay, W. R. Wadt, *J. Chem. Phys.* **1985**, *82*, 270.
[52] W. R. Wadt, P. J. Hay, *J. Chem. Phys.* **1985**, *82*, 284.
[53] P. J. Hay, W. R. Wadt, *J. Chem. Phys.* **1985**, *82*, 299.
[54] K. Riley, K. Merz, *J. Phys. Chem., A* **2007**, *111*, 6044.
[55] S. F. Boys, F. Bernardi, *Mol. Phys.* **1970**, *19*, 553.
[56] J. B. Foresman, T. A. Keith, K. B. Wiberg, J. Snoonian, M. J. Frisch, *J. Phys. Chem.* **1996**, *100*, 16098.
[57] C. M. Breneman, K. B. Wiberg, *J. Comput. Chem.* **1990**, *11*, 361.
[58] F. C. McElroy, J. C. Dabrowiak, *J. Am. Chem. Soc.* **1976**, *98*, 7112.
[59] M. Villagran, J. P. Muena, J. Costamagna, J. Zagal, A. G. Lappin, G. Ferraudi, *Inorg. Chim. Acta* **2009**, in press, doi: 10.1016/j.ica.2008.09.051.

Received August 13, 2008